International Journal of New Technology and Research (IJNTR)
ISSN:2454-4116, Volume-2, Issue-2, February 2016 Pages 85-95

Statistics Analysis of Anomalous Signals Prior to Large Earthquakes

Weihang Huang, Wen-Bin Shen, Wenqiang Zhang, Xiang Gu, Tianxing Jiang

***Abstract*—Anomalous signals prior to large earthquakes might be detected based on superconducting gravimeters (SGs) and broadband seismometers (BSs) records. In this study, we selected 12 large earthquakes with their seismic magnitudes larger than 7.8, occurred between 2006 and 2010. Hilbert-Huang transform (HHT) technique, which is applicable for nonlinear and non-stationary processes, was applied to SG record and BS data sets sampled at one-second interval covering the time span 7 days prior to and 1 day after these earthquakes. Our study shows that anomalous signals are likely to occur in any one of the several days prior to large earthquakes. The results based on the SG record show that the anomalous signals with dominant frequency around 0.13 Hz occur 16 hours to 5 days prior to the large earthquake. Whereas records from 48 BS station suggest four obvious intrinsic frequency bands, namely around 0.06Hz, 0.33Hz, 0.43Hz and 0.46Hz, respectively. Concerning the BS records, the anomalous signals are characterized by total increase of the energy of signals and the anomalous peaks of the marginal spectra around 0.15-0.2 Hz and 0.33 Hz.**

***Index Terms*—large earthquake, anomalous signals, superconducting gravity data, broadband seismic data, Hilbert-Huang transform.**

I. INTRODUCTION

For the purpose of earthquake prediction study, numerous studies **Error! Reference source not found.**–[10] addressed different kinds of anomalous phenomena before large earthquakes. Previous studies [11]–[14] suggested that, superconducting gravimeters (SGs) [15],[16] and broadband seismometers (BSs) can detect anomalous signals prior to large earthquakes. For instance, anomalous signals were found prior to 2008 Wenchuan Mw7.9 earthquake and 2010 Peru Mw9.0 earthquake.

This study selects twelve large earthquakes with their seismic magnitudes being larger than 7.8 that occurred between 2006 and 2010. We apply Hilbert-Huang transform (HHT) technique [17] to SG data and BS data that cover the time span seven days prior to and one day after these earthquakes and then analyze anomalous signals prior to large earthquakes and provide their time-frequency-energy spectra. Fig.1 shows the distribution of the selected twelve large earthquake events and the SG station. Almost all of the twelve large earthquakes are located at plate boundaries. And the information in details of the selected large earthquakes is listed in Table 1.

Weihang Huang, Institute of Geology and Geophysics, Chinese Academy of Sciences, Beijing, China, 86-13126678840,

Wen-Bin Shen, Department of Geophysics, School of Geodesy and Geomatics, Wuhan University, Wuhan, China, 86-18908628627

Wenqiang Zhang, School of Earth and Space Sciences, University of Science and Technology of China, Hefei, China, 86-18856032206

Xiang Gu, School of Finance, Shanghai University of Finance and Economy, Shanghai, China, 86-17717623932

Tianxing Jiang, School of Earth and Space Exploration, Arizona State University, Tempe, US, 1-4807381152

Correspondence: Wen-Bin Shen. This study is supported by National 973 Project China (grant No. 2013CB733305), NSFC (grant Nos. 41174011, 41574007, 41128003, 41210006 , 41021061, 40974015).

II. DATA AND METHOD

A. Data and Preprocessing

The data adopted here are SG and BS data sampled at one-second interval covering the time span 7 days prior to and 1 day after these earthquakes. We note that only for the great earthquake events whose magnitudes are equal to or larger than Mw9.0, the one-second interval SG data before and after the events for one month are available from the data center of Global Geodynamic Project (GGP), and for other earthquake events, GGP provides only one-min interval SG data continuously. However, one-min interval data can only be used for resolving signals at frequencies smaller than 0.01Hz. Hence, here we use one-second interval SG data between 2006 and 2010 at HS (Hsinchu, Taiwan) station. In addition, we used one-second interval seismic data (LHZ) from 48 BS stations during the period 2006 to 2010, which are accessible in the data center of Incorporated Research Institutions for Seismology (IRIS, http://www.iris.edu/data/). For the seismic stations, we chose stations located in the range with their epicentral distances being smaller than 2000 km according to different earthquakes.

Both SG data and BS data need preprocessing. The specific processes are stated as follows.

Tidal effects should be removed from the original SG data before further analysis [18]. This process is completed by using the software T-soft provided by the International Center for Earth Tides (ICET, http://www.astro.oma.be/ICET), in which the theoretical value of solid tide is computed by the solid tide model based on the specific location and elevation of each station. Fig.2 shows an example of the preprocessing in removing tidal effects from the SG record at HS station.

Fig.2a shows the original SG data, Fig.2b shows the tide model, which can be computed by the tide parameters at the SG location, and Fig.2c shows the residual SG series after removing the tidal effects. The data processing procedures could be summarized as follows: first, multiply the original observations by a coefficient (which is provided by the SG data file) to get the gravity observations (Fig.2a); then, subtract the tide model (Fig.2b) from the gravity

Table 1. Information of the large earthquakes with a seismic magnitude being larger than 7.8 that occurred between 2006 and 2010.

Earth quake	Date	Time	Magnitude	Region	Longitude	Latitude	Depth (km)	Typhoon duration &name
1	2006.05.03	15:26:39	Mw7.9	Tonga Islands	-174.14	-20.16	53.5	None
2	2006.11.15	11:14:14	Mw8.3	Kuril Islands	153.21	46.68	12.2	11.9-11.13 CHEBI
3	2007.01.13	4:23:23	Mw8.1	East of Kuril Islands	154.5	46.23	22.5	None
4	2007.04.01	20:39:56	Mw8.1	Solomon Islands	157.03	-8.45	9.5	4.1-4.6 KONG-REY
5	2007.09.12	11:10:26	Mw8.5	Southern Sumatera	101.4	-4.46	35.5	8.29-9.8 FITOW 9.7-9.11 DANAS
6	2007.12.09	7:28:20	Mw7.8	South of Fiji Islands	-177.36	-26.1	149.8	None
7	2008.05.12	6:27:59	Mw7.9	Wenchuan, China	103.37	31.06	7.6	5.7-5.13 RAMMASUN
8	2009.07.15	9:22:31	Mw7.8	Off W. Coast of S. Island, Newzealand	166.64	-45.83	20.9	7.11-7.12 SOUDELOR
9	2009.09.29	17:48:00	Mw8.1	Samoa Islands Region	-171.94	-15.51	18.5	9.26-9.30 KETSANA
10	2009.10.07	22:18:53	Mw7.8	Santa Cruz Islands	166.37	-12.47	59	9.29-10.14 PARMA 9.30-10.08 MELOR
11	2010.04.06	22:15:02	Mw7.8	Northern Sumatera	97.11	2.36	33.4	None
12	2010.10.25	14:42:22	Mw7.8	Southern Sumatera	100.1	-3.52	20	10.13-10.23 MEGI 10.24-10.30 CHABA

(http://agora.ex.nii.ac.jp/digital-typhoon/search_date.html.en#id2
http:// www.iris.edu/SeismiQuery/breq_fast.Phtml)

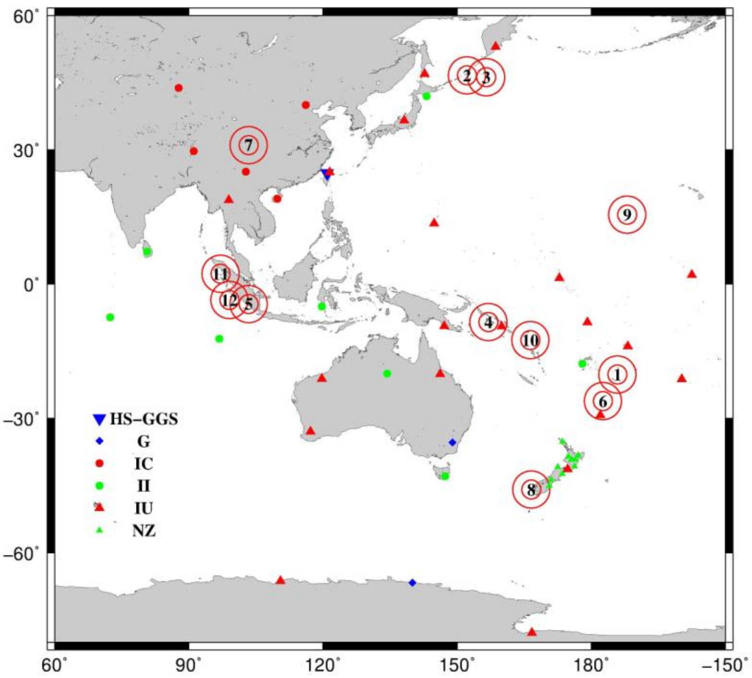

Figure 1 Distribution of large earthquakes events, the SG station (denoted by a blue triangle) and the BS stations (denoted by other figuration symbols). Numbers 1-12 represent respectively twelve large earthquakes with a seismic magnitude being larger than 7.8 that occurred between 2006 and 2010. HS-GGS. Hsinchu, Taiwan; G. GEOSCOPE (GEOSCOPE); IC. New China Digital Seismograph Network (NCDSN); II. Global Seismograph Network (GSN-IRIS/IDA); IU. Global Seismograph Network (GSN-IRIS/USGS); NZ. New Zealand National Seismograph Network(GNS New Zealand).

observations to obtain the residual SG series (Fig.2c), which will be further used for the purpose of detecting anomalous signals prior to large earthquakes. Here we note that, by various experiments, for the present purpose, other corrections (e.g. pressure influence, polar tide effect etc.) are not necessary.

The BS data from IRIS website is in the seed format, which is a kind of format that exclusively stores seismic data.

The software rdseed in the IRIS can be used to transfer the seed file to binary SAC (Seismic Analysis Code) file, which

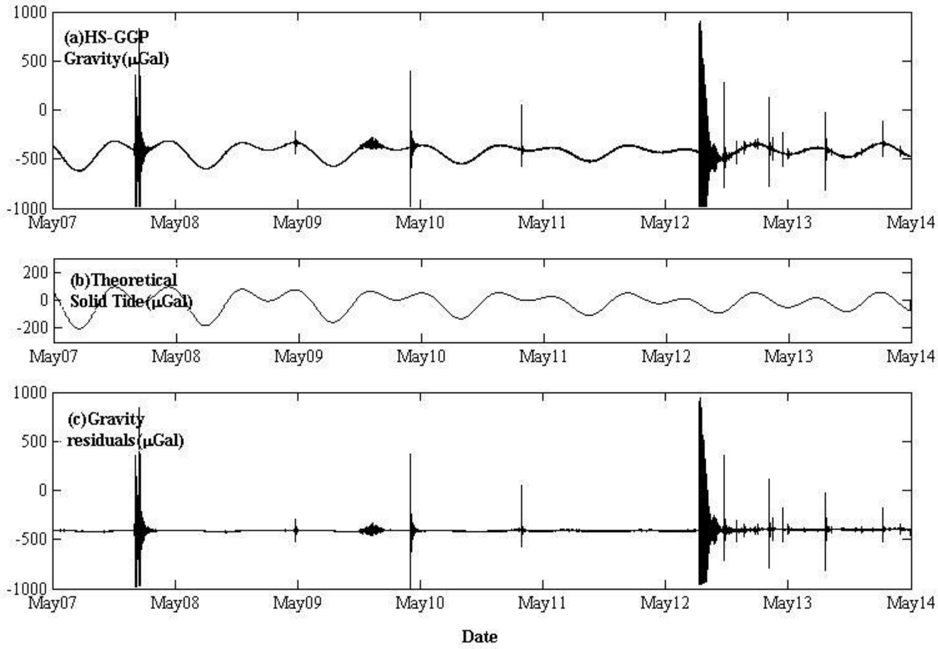

Figure 2 The preprocessing using the software T-soft to remove the tidal effects. (a) Original one-second SG records at HS station; (b) theoretical values of tides; (c) residual SG series after removing the tidal effects.

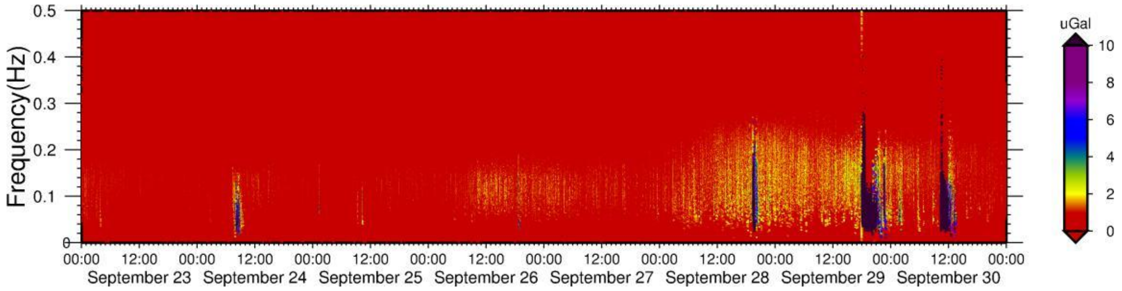

Figure 3 HHT spectrum of SG data series that cover the period September 23-30, 2009 at HS station, and in this period an earthquake with magnitude of 8.1 occurred at 17:48:00 on Sept.29, located at -171.94°,-15.51°.

is further processed by the SAC software.

The SAC software is developed by Lawrence Livermore National Laboratory (LLNL) at University of California and is extensively used to process and study time series signals, especially seismic signals. The function of this software includes general arithmetic operation, Fourier transform, spectrum estimation, IIR and FIR filtering-signal stacking, data extraction, interpolation, correlation analysis, seismic phase picking and so on. SAC uses driving mode of interactive commands, which means each command should either be input in the terminal or be put in the macro file to be executed. Applying the SAC software is the first step in processing seismic data in this study. Just simply using the function transfer one can take a derivative of time series two times to generate time series expressed in acceleration form.

B. Method

This study applies the HHT technique, which is applicable for nonlinear and non-stationary time series, to process SG data and BS data. The key of the method is the empirical mode decomposition (EMD) with which any complicated data set can be decomposed into a finite and often small number of intrinsic mode functions (IMFs) [17], [19], [20]. An intrinsic mode function (IMF) is a function that satisfies two conditions [17]: (1) in the whole data set, the number of extrema and the number of zero crossings must either equal or differ at most by one; and (2) at any point, the mean value of the envelope defined by the local maxima and the envelope defined by the local minima is zero. Based on this approach a complicated time series can be effectively decomposed into several IMF components which are arrayed from high frequency to low frequency.

After obtaining the IMF components, one can apply Hilbert transform to each component and compute the instantaneous frequency and instantaneous amplitude at any moment [21], thus construct the energy-frequency-time distribution, designated as HHT spectrum [22]. From the computing process, HHT method is a kind of spectrum analysis technique with fine time resolution and locality, which works great for non-stationary time series and might be valid for anomalous signals detection prior to earthquakes [13].

To get more clear relationship between the amplitude and frequency of anomalous signal, we can also look at the marginal spectrum. It represents the total amplitude contribution from each frequency value in a certain time period. If HHT spectrum is expressed as $H(t, f)$, where t denotes time, f denotes frequency, H denotes amplitude, then the marginal spectrum is defined as

$$h(f)=\int H(t, f)dt \tag{1}$$

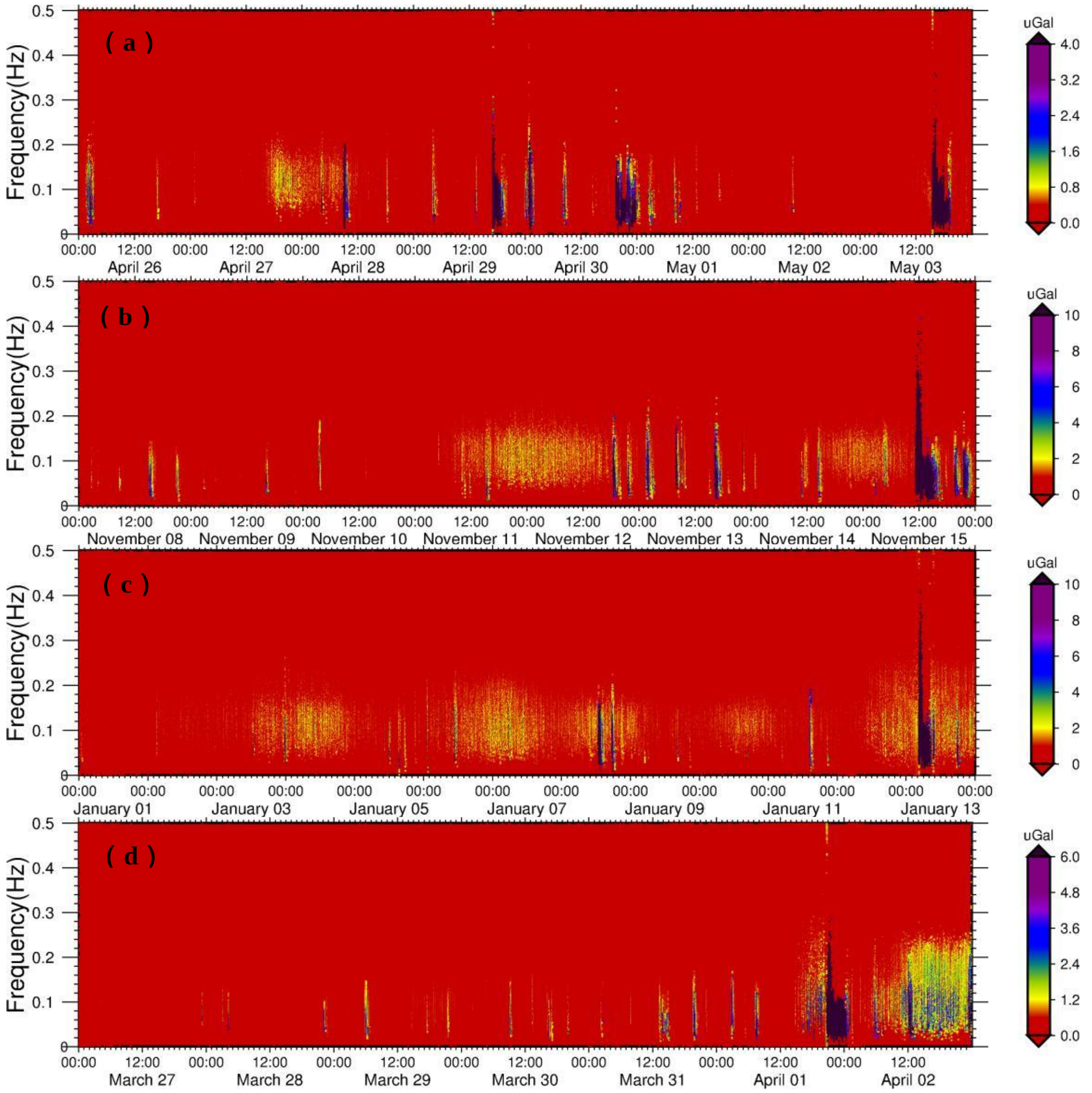

Figure 4 (a) HHT spectrum of SG data series that cover the period April 26 to May 3, 2006 at HS station, and in this period an earthquake with a magnitude of 7.9 occurred at 19:26:39 on May 3 , located at -174.14°, -20.26° (see Table 1); (b) HHT spectrum of SG data series that cover the period November 8-15, 2006 at HS station, and in this period an earthquake with a magnitude of 8.3 occurred at 11:14:14 on November 15 , located at 153.21°, 46.68° (see Table 1); (c) HHT spectrum of SG data series that cover the period January 1-13, 2007 at HS station, and in this period an earthquake with a magnitude of 7.9 occurred at 4:23:23 on January 13, located at 154.5°, 46.23° (see Table 1); (d) HHT spectrum of SG data series that cover the period Mar 27 to April 2, 2007 at HS station, and in this period an earthquake with a magnitude of 8.1 occurred at 20:39:56 on April 1, located at 157.03°, -8.45° (see Table 1).

It is necessary to compare the marginal spectra of different time periods with different lengths. So we divide the marginal spectrum by the length of the time period T , as

$$h(f)=\left(\int H(t, f)dt\right)/T \tag{2}$$

Strictly speaking, what we compute and apply here is actually the average marginal spectrum (simply referred to marginal spectrum hereafter for convenience) [13]. And considering various shapes of the marginal spectrum at each station, the marginal spectra are normalized before they are compared to highlight the features of anomalous signals. Normalized marginal spectra here is defined as

$$h_n(f)=h(f)/h_{\max}(f) \tag{3}$$

III. Result and Analysis

A. Anomalous signal detected by SG data

HHT spectrum of SG data at HS station is shown in Fig.3. HHT spectrum clearly shows that the amplitudes corresponding to specific frequency bands have abnormal increase. From Fig.3, a small earthquake occurred one day before the large earthquake, and the anomalous signals with dominant frequency around 0.1Hz occurred thirteen to six hours prior to the large earthquake. And in the study on Wenchuan earthquake, similar anomalous signals have been detected two days prior to the large earthquake [13]. Hence we may suggest that the signals detected here are possibly the anomalous signals related to the large earthquake.

However, by carefully examining a few large earthquakes, we found that sometimes the anomalous signals appear 4-5 days prior to large earthquakes, with dominant frequency around 0.1Hz, as shown in Fig.4. Therefore, here

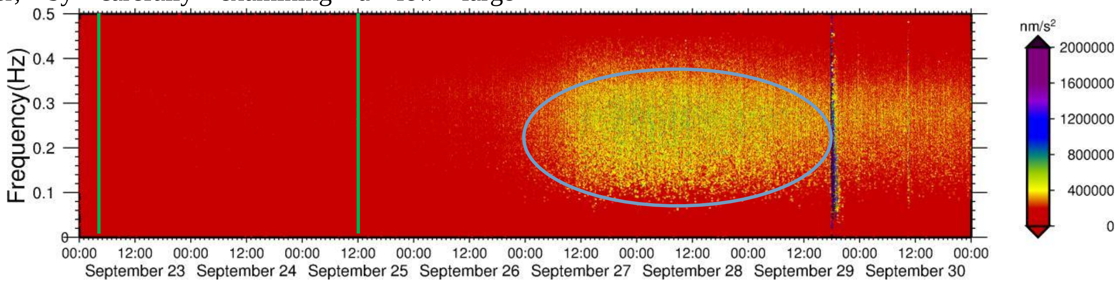

Figure 5 HHT spectrum of BS data series that cover the period September 23-30,2009 at RPZ (NZ) station, and in this period an earthquake with a magnitude of 8.1 occurred at 17:48:00 on September 29, located at -171.94°, -15.51° (see Table 1). The two vertical green solid lines mark the quiet days when the amplitudes are small and steady, and the blue ellipse marks the anomalous days when the amplitudes have an obvious increase. In HHT spectrum of BS data series below, the two symbols are also used to mark the quiet days and anomalous days.

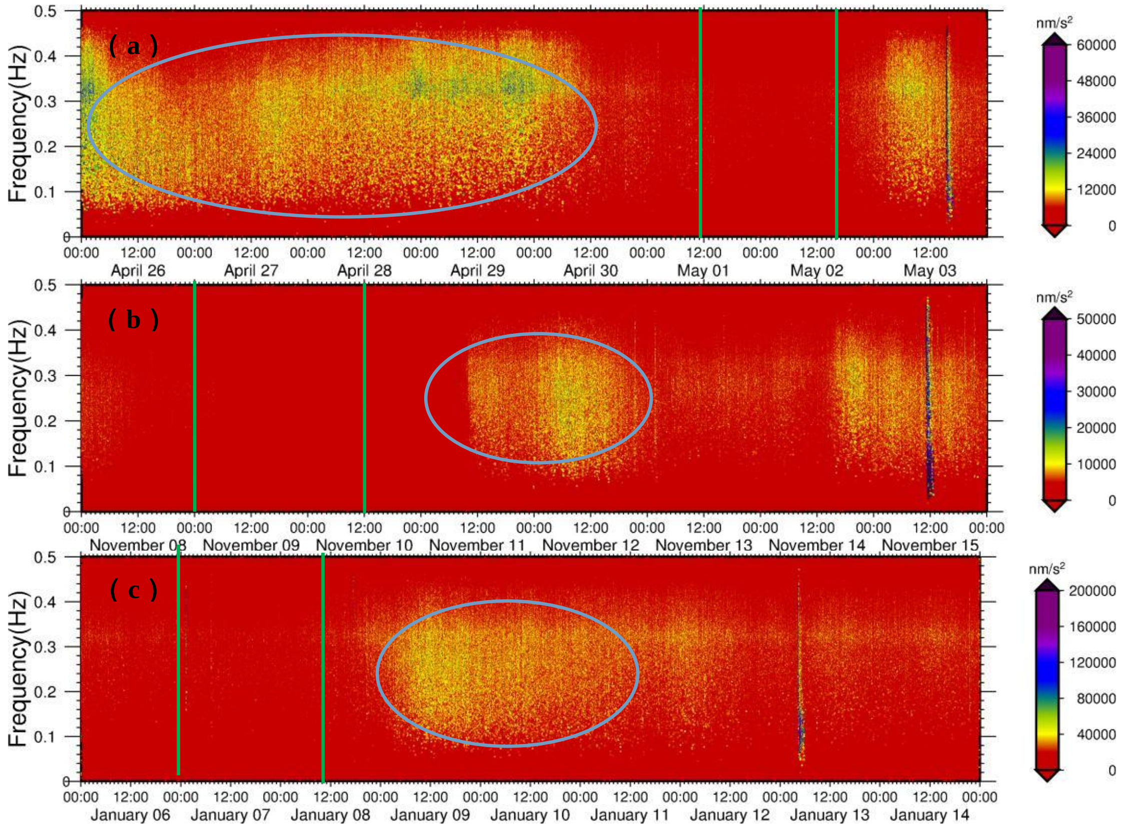

Figure 6 (a) HHT spectrum of BS data series that cover the period April 26 to May 3, 2006 at SNZO(IU) station, and in this period an earthquake with magnitude of 7.9 occurred at 15:26:39 on May 3, 2006, located at -174.14°, -20.26° (see Table 1); (b) HHT spectrum of BS data series that cover the period November 8-15, 2006, at MAJO (IU) station, and in this period an earthquake with magnitude of 8.3 occurred at 11:14:14 on November 15, 2006, located at 153.21°,46.68° (see Table 1); (c) HHT spectrum of BS data series that cover the period January 1-13, 2007 at HS station, and in this period an earthquake with magnitude of 7.9 occurred at 4:23:23 on January 13, 2007 located at 154.5°, 46.23° (see Table 1).

we might suggest that many factors may contribute to SG records. For instance, an earthquake with a relatively small magnitude and a short distance can result in an abnormal increase in the amplitude of HHT spectrum in the records, and it even submerges the anomalous signals related to the large earthquake.

B. HHT spectrum of BS records

Applying HHT method to BS data will generate an energy-frequency-time distribution, as shown by Fig.5. From Fig.5, prior to large earthquakes, some broadband seismometers are able to detect the signals with abnormal increases in amplitude, which has been shown in the previous studies [11], [13]. But, via statistical analysis of a few large earthquakes, we found that anomalous signals may occur several hours to several days prior to large earthquakes as shown in Fig.6 other than around two days prior to the events as suggested by [13]. Similar phenomenon has been pointed out by [11].

As shown by Fig.6a, the anomalous signals detected at

SNZO (IU) station occurred 4-5 days before the large 2006 Kuril Islands earthquake Mw8.3 event; in Fig.6b, the anomalous signals detected at MAJO (IU) station occurred 3-4 days before the event; and in Fig.6c, the anomalous signals detected at GUMO (IU) station occurred 2-4 days before the event.

In all of the figures of HHT spectra of BS data series, the situation is similar, and that is to say, the occurrence time of the anomalous signals varies and has certain random nature. But a closer look at the HHT spectra shows that the

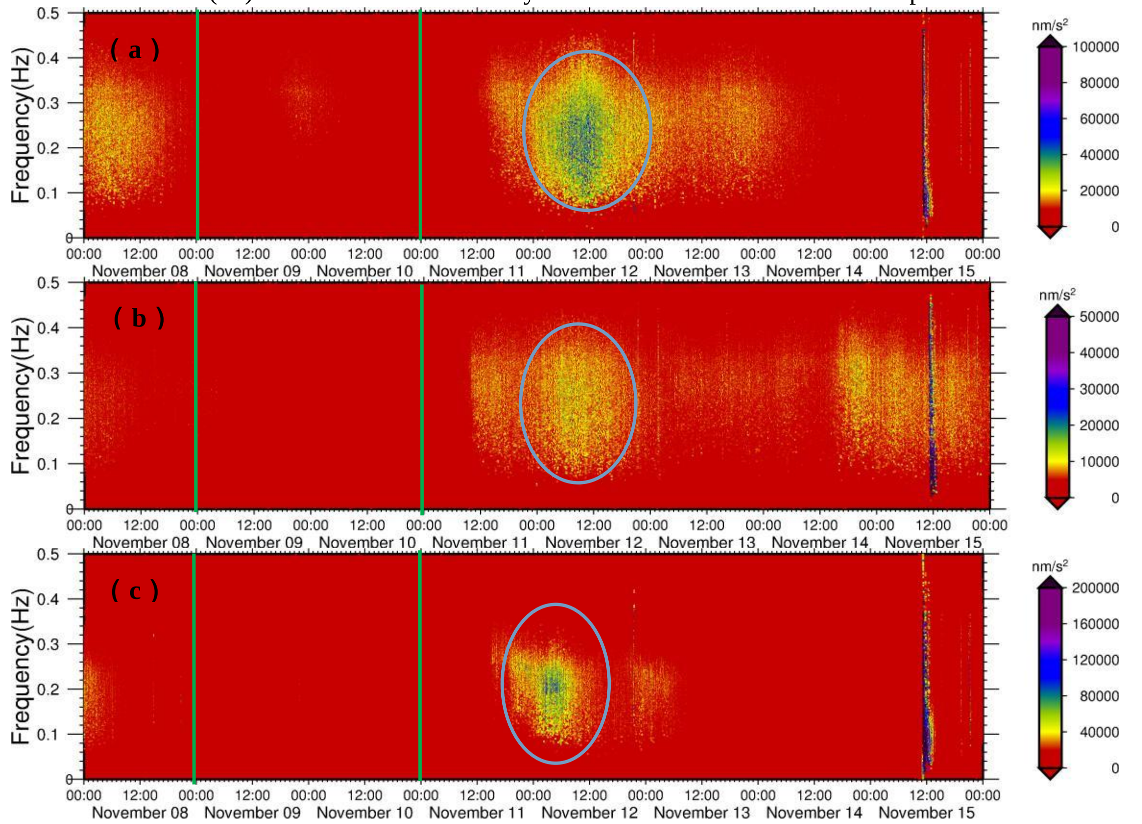

Figure 7 HHT spectra of BS data series that cover the period November 8-15, 2006 at several different stations, and in this period an earthquake with magnitude of 8.3 occurred at 11:14:14 on November 15, 2006, located at 153.21°, 46.68° (see Table 1).

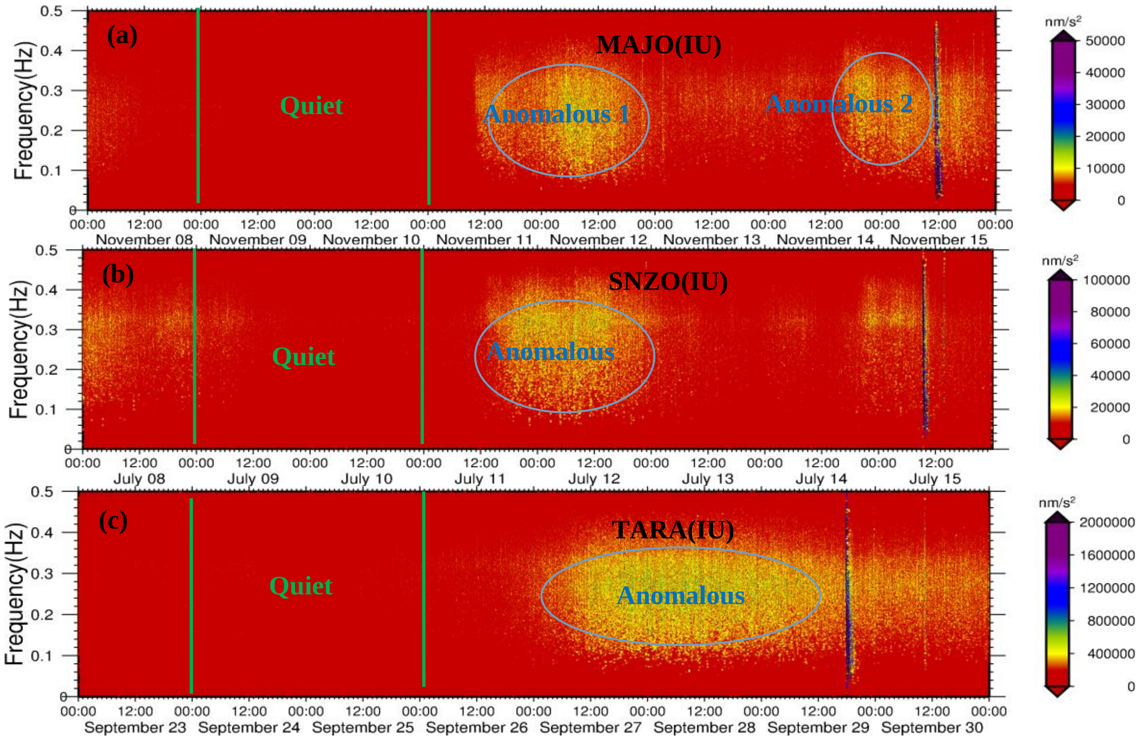

Figure 8 HHT spectra of the BS data before and after three typical seismic events selected to analyze the differences of the characteristics of the signals between the quiet days (denoted by two vertical green solid lines) and anomalous days (denoted by

the blue ellipses). The time of these events is: (a) November 15, 2006; (b) July 15, 2009; (c) September 29, 2009. The seismic stations have been marked in the figures.

anomalous signals detected at different stations related to the same earthquake occurred almost in the same time period, as shown in Fig.7.

Fig.7 suggests that at YSS(IU) station (see Fig.7a), MAJO(IU) station (see Fig.7b) and ERM(II) station (see Fig.7c) the anomalous signals are detected on the early morning of November 1. And the energy-frequency distributions of the anomalous signals in HHT spectra are

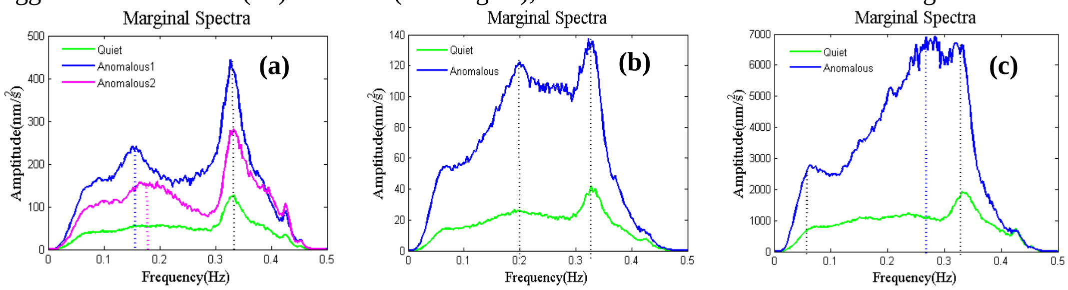

Figure 9 The marginal spectra based on BS records in the quiet days (denoted by green solid lines) and anomalous days (denoted by blue or purplish red solid lines). (a) November 8-15, 2006, MAJO (IU); (b) July 8-15, 2009, SNZO (IU); (c) September 22-30, 2009, TARA (IU)

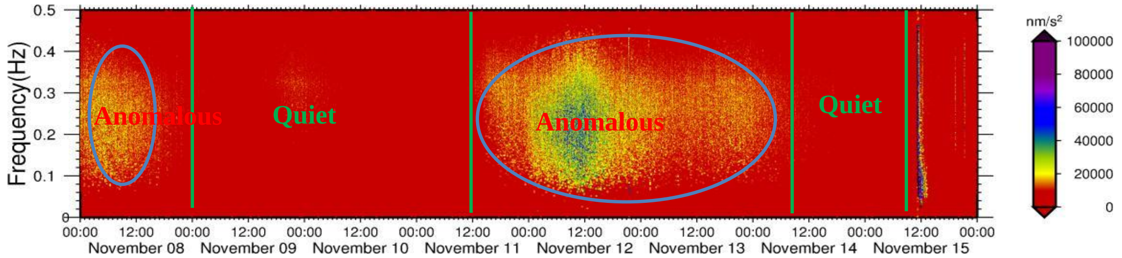

Figure 10 HHT spectrum of the seismic records at YSS station (IU) that covers the period November 8-15, 2006.

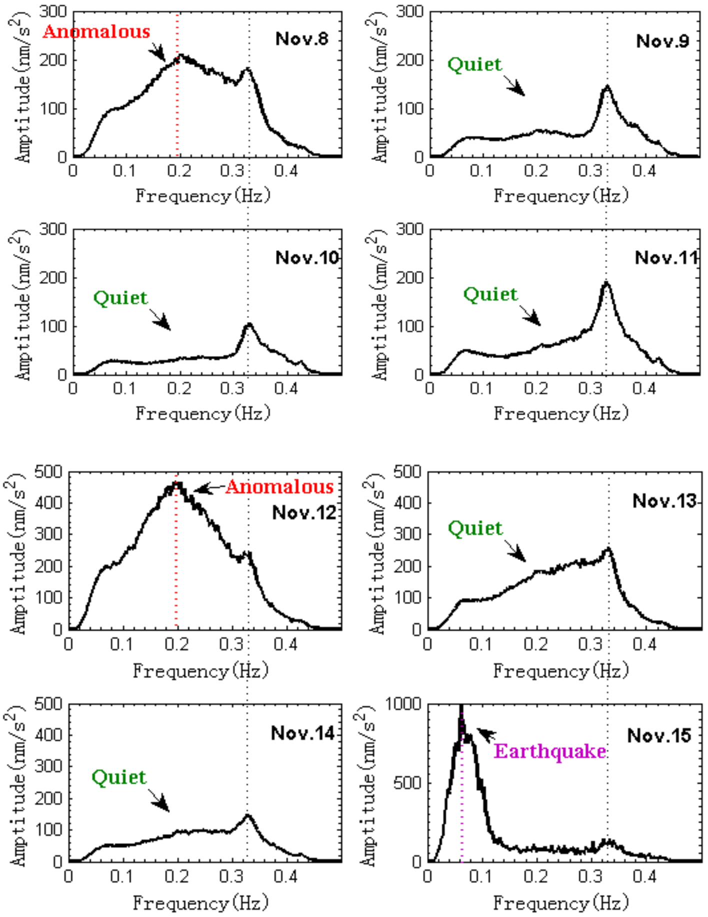

Figure 11 Segmented marginal spectra of seismic records at YSS station (IU) that covers the period November 8-15, 2006.

also similar. Hence, the detected signals may result from the same cause. Considering that these three stations are all located close to the epicenter of the 2006 Kuril Islands Mw8.3 earthquake, we might conclude that the anomalous signals should be caused by this earthquake.

C. Comparison of the signals based on BS records between the quiet days and anomalous days

As mentioned above, anomalous signals may occur 1-2 days or 3-4 days before the earthquake. Nevertheless, we can always distinguish the quiet days from the anomalous days in HHT spectrum 6-7 days prior to the large earthquake. We selected three typical earthquake events in order to analyze the difference of the characteristics of the signals between the quiet days and anomalous days. Fig.8 shows HHT spectra and the chosen quiet days and anomalous days. Then we computed the marginal spectra in these two periods,

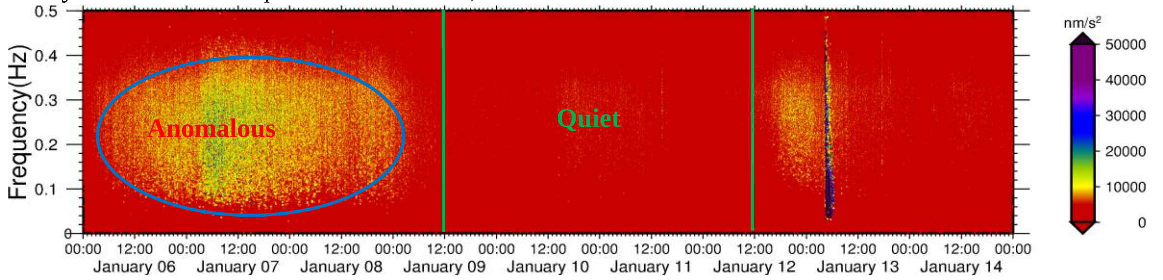

Figure 12 HHT spectrum of the seismic records at GUMO station (IU) that covers the period January 1-13, 2007.

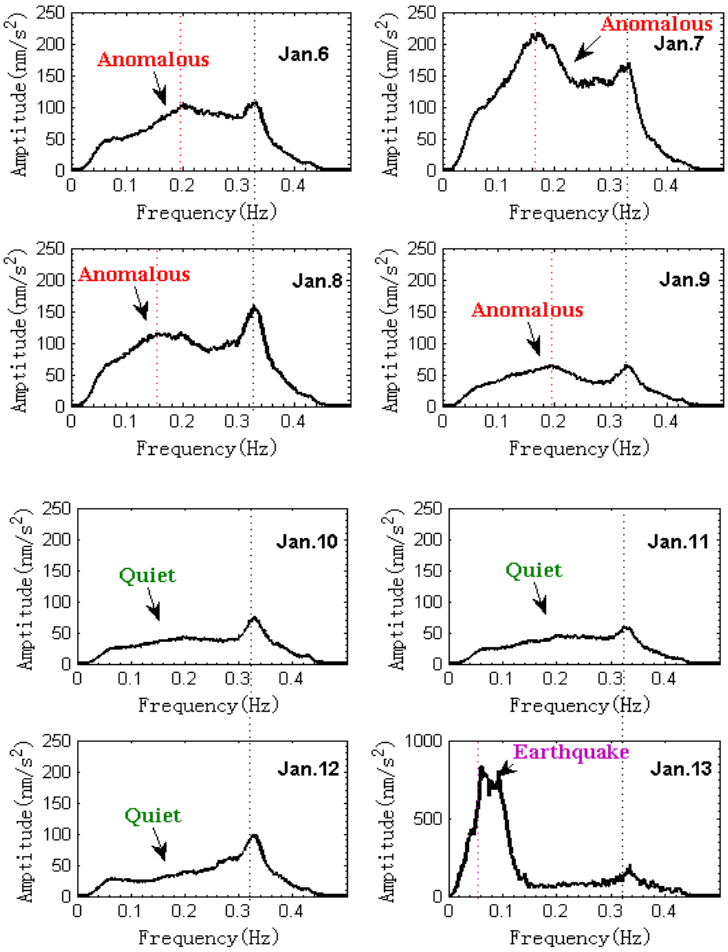

Figure 13 Segmented marginal spectra of seismic records at YSS station (IU) that covers the period January 1-13, 2007.

respectively, as shown in Fig.9.

From Figs.8 and 9 we find that, compared to signals in the quiet days, the amplitudes of the anomalous signals increase obviously, and the marginal spectra have a peak around 0.2Hz in the frequency domain. Meanwhile, the amplitudes of the signals in both periods have a peak around 0.33Hz, which is very likely to be the intrinsic frequency band of the BS records, caused by other factors but earthquake. Hence, for the convenience of our discussion, we define the peak around 0.33Hz as the intrinsic peak while name the peak around 0.2Hz as the anomalous peak.

As Fig.9a shows, there are two different dominant frequencies of the signals, 0.15Hz and 0.18Hz, in two anomalous periods prior to earthquakes, which indicates that the dominant frequency of the anomalous signals is not stable and can vary within a certain band (usually it is very close to 0.2Hz). In Fig.9b, the marginal spectrum in the quiet days has a weak peak around 0.2Hz. Obviously, the definition of quiet days should not be taken in an absolute sense but a relative sense [13]. There might be some weak anomalous signals mixed in quiet days. Another fact we should notice is that the dominant frequency of the anomalous signals is not always very close to 0.2Hz, whereas the dominant frequency is close to 0.28Hz, as shown in Fig.9c. From Fig.8, the anomalous signals at TARA station occurred closer to the earthquake event in term of time. So in some sense the anomalous signals are random and complicated. Further investigations are needed.

D. Analysis of segmented marginal spectra based on seismometers records

In order to further investigate the characteristics of the signals in both the quiet days and anomalous days, we selected single earthquake event and computed the segmented marginal spectra in each day.

Taking the 2006 Kuril Islands Mw8.3 earthquake event for example, we computed HHT spectrum of the seismic records at YSS station (IU), as shown in Fig.10. And the segmented marginal spectra are shown in Fig.11.

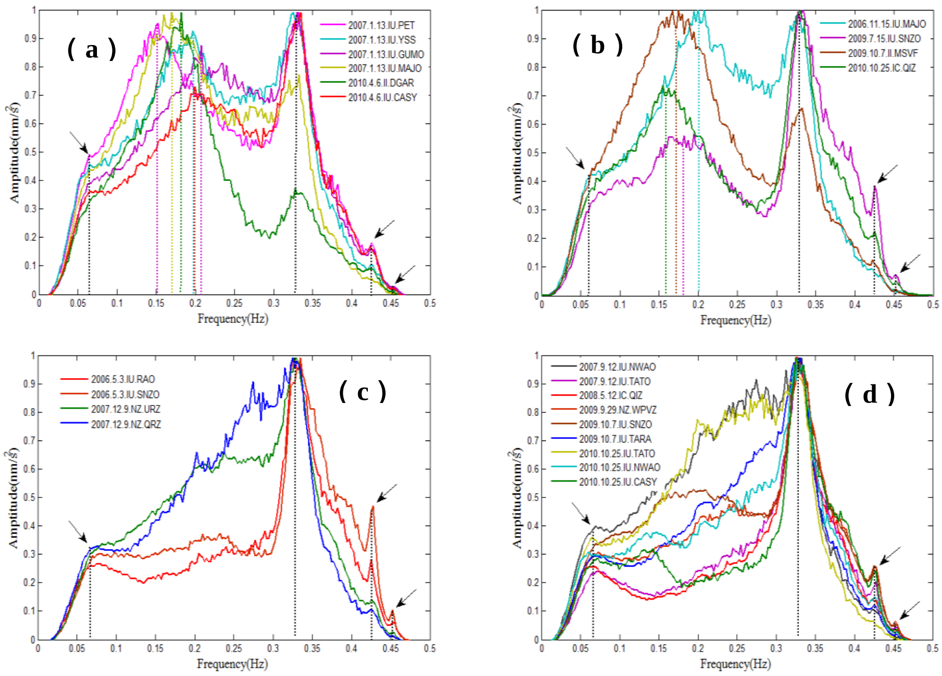

Figure 14 Marginal spectra of the seismic records in the anomalous days among 48 BS stations. (a) Marginal spectra of the records where the dominant frequency are aournd 0.2 and 0.33 Hz without typhoon influence; (b) Marginal spectra of the records where the dominant frequency are around 0.2 and 0.33 Hz with typhoon influence; (c) Marginal spectra of the records where the dominant frequency is only 0.33 Hz without typhoon influence; (d) Marginal spectra of the records where the dominant frequency is only 0.33 Hz with typhoon influence. Solid arrows show a sharp peak around 0.43Hz, a small sharp peak around 0.46Hz and a small side lobe around 0.07Hz. Information of anomalous period of the relevant stations is provided in the sequel: (a)PET(2007.1.8.0h-2007.1.9.0h),YSS(2007.1.7.0h-2007.1.8.0h),GUMO(2007.1.9.6h-2007.1.9.0h),MAIO(2007.1.7.0h-2007.1.8.0h),DGAR(2010.4.4.12h-2010.4.5.12h),CASY(2010.4.18.h-2010.5.18h);(b)MAJO(2006.11.12.0h-2006.11.12.18h),SNZO(2009.7.11.18h-2009.7.12.18h),MSVF(2009.10.5.20h-2009.10.6.20h),QIZ(2010.10.20.12h-2010.10.21.12h);(c)RAO(2006.4.29.12h-2006.4.30.12h),SNZO(2006.4.29.0h-2006.4.30.0h),URZ(2007.12.4.0h-2007.12.6.0h),QRZ(2007.12.4.12h-2007.12.6.12h);(d)NWAO(2007.9.7.12h-2007.9.8.12h),TATO(2007.9.11.0h-2007.9.12.0h),QIZ(2008.5.10.12h-2008.5.12.0h),WPVZ(2009.9.23.0h-2009.9.24.12h),SNZO(2009.10.3.0h-2009.10.6.0h),TARA(2009.10.3.0h-2009.10.6.0h),TATO(2010.10.23.6h-2010.10.24.0h),NWAO(2010.10.23.6h-2010.10.20.6h),CASY(2010.10.19.18h-2010.10.20.18h).

Fig.10 demonstrates that anomalous signals occur in November 8, 12 and 13. And we can find a peak around 0.2Hz in November 8 and 12 at segmented marginal spectra in Fig.11. The time period of the anomalous signals occurrence as shown by the HHT spectrum agrees with that as shown by the marginal spectra, and the dominant frequencies of the anomalous signals as shown by both the HHT spectrum and the marginal spectra are very close to each other.

Now we consider the Kuril Islands Mw8.1 earthquake event occurring in January1-13, 2007. After computing HHT spectrum and the marginal spectra we can find that the anomalous signals occurred in January 6-8, as shown in Fig.12. And the marginal spectra have anomalous peaks around 0.2Hz on January 6-9, as shown in Fig.13. Besides, the dominant frequencies of the anomalous signals on January 6-9 are 0.2Hz, 0.16Hz, 0.15Hz and 0.2Hz, respectively.

E. Detailed analysis on the characteristics of the marginal spectra based on seismometers records in the anomalous days

Since most earthquake events that we selected occurred along the coast of western Pacific (see Fig.1), where many typhoons happened in the whole year. Considering this fact, typhoon events are critical factors that might disturb the anomalous signals detection.

We divided these earthquake events which occurred in 2006-2010 into two groups:

Group I: there are 4 seismic events which were not affected by typhoon events, namely, 3 May 2006 Mw7.9 event, 13 January 2007 Mw8.1 event, 9 December 2007 Mw7.8 event, 6 April 2010 Mw7.8 event (see Table 1).

Group II: there are 8 seismic events (see Table 1) which might be disturbed by typhoon events (including 2006 CHEBI, 2007 KONG-REY & FITOW & DANAS, 2008 RAMMASUN, 2009 SOUDELOR & KETSANA & PARMA & MELOR, 2010 MEGI & CHABA) (see Table 1, and Fig.15).

As mentioned before, we can distinguish the anomalous days from the quiet days in HHT spectrum 6-7 days prior to the large earthquake. Here we choose such days which have obvious anomalous signals and then focus on the comparison of the characteristics of these signals between two groups above to reveal more detailed information.

A previous study [13] has suggested two patterns of the energy-frequency distributions. One pattern comes from the records of inland seismic stations, which has only one peak around 0.33Hz in the marginal spectra. And the other pattern comes from the records of coastal seismic stations, which has two peaks around 0.2Hz and around 0.33Hz. Accordingly, we classified the anomalous signals which come from different events and different stations including the possible influences of typhoon events. For the detailed analysis on the anomalous signals, we normalized every marginal spectrum and plotted them together in one figure (Fig.14). Then more detailed characteristics are shown (pay attention to those arrows marked in Fig.14).

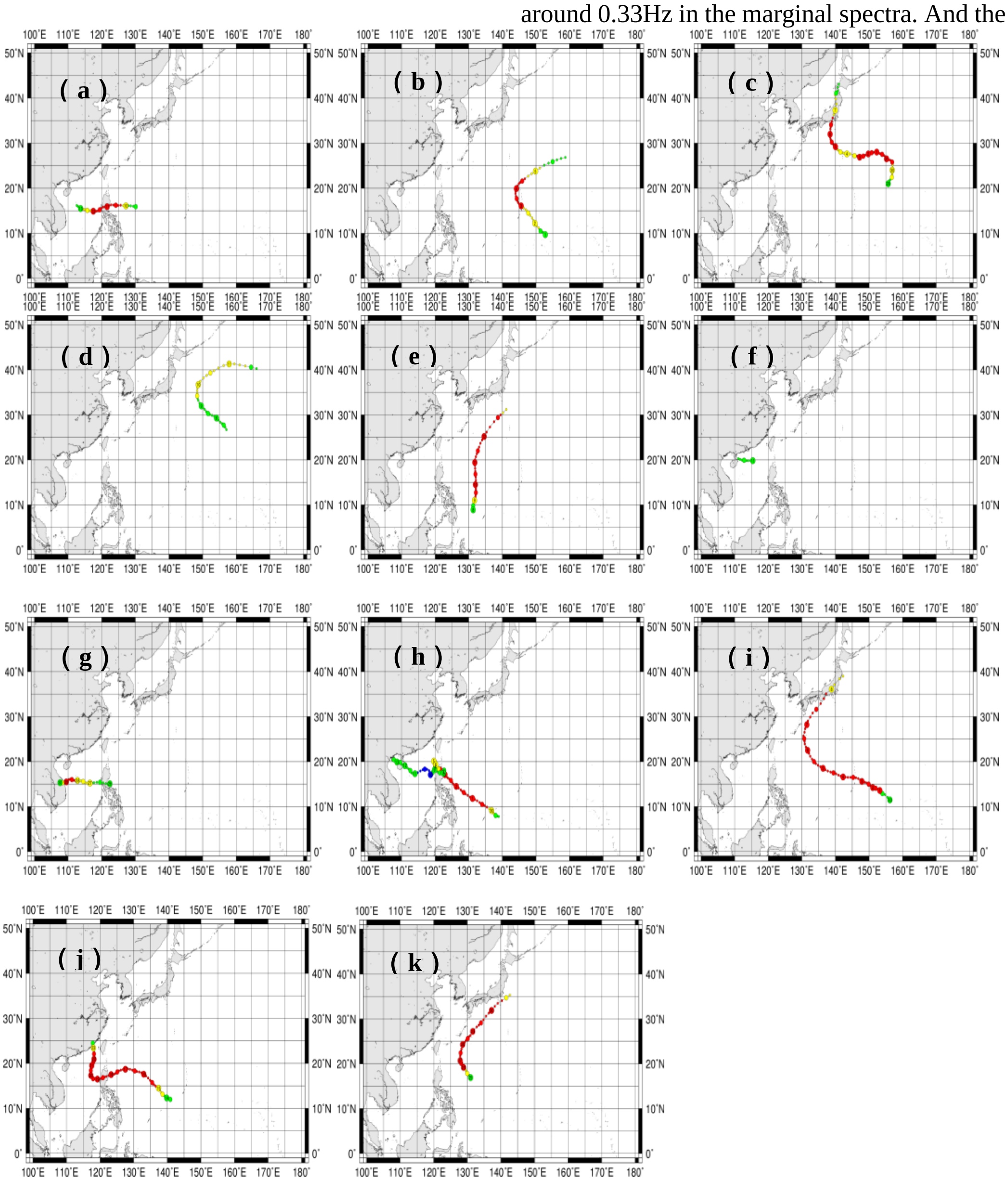

Figure 15 Typhoon events and their paths. (a) 2006 CHEBI; (b) 2007 KONG-REY; (c) 2007 FITOW; (d) 2007 DANAS; (e) 2008 RAMMASUN; (f) 2009 SOUDELOR; (g) 2009 KETSANA; (h) 2009 PARMA; (i) 2009 MELOR; (j) 2010 MEGI; (k) 2010 CHABA.
(http://agora.ex.nii.ac.jp/digital-typhoon/search_date.html.en#id2)

All of the Figs.14a (group I), 14b (group II), 14c (group I) and 14d (group II) show two peaks in their marginal spectra. However, carefully examining each subfigure of Fig.14, we found that there are no obvious differences in the energy-frequency distributions between group I and group II. We can find some other common features in these four subfigures, besides the common characteristics we have mentioned above (the peak around 0.33Hz). To be specific, we observed a sharp peak around 0.43Hz, a small sharp peak around 0.46Hz and a small side lobe around 0.07Hz in all the marginal spectra. We consider that these four features are the intrinsic frequency bands contained in the seismic data which have nothing to do with the anomalous signals prior to large earthquakes.

In addition, the amplitudes around 0.15-0.2Hz in Figs.14a and 14b are similar and the amplitudes around 0.15-0.23Hz in Figs.14c and 14d are similar, too. Hence, we conclude that the typhoon may not give rise to the anomalous signals around 0.2Hz.

IV. Discussions and Conclusions

By applying HHT analysis method to SG data and BS data, and examining the normalized marginal spectra, we found that the SG records show that the anomalous signals with dominant frequency around 0.13 Hz occur 16 hours to 5 days prior to the large earthquake. However, BS records have four obvious intrinsic frequency bands: the 0.33Hz main peak, the 0.43Hz sharp peak, the 0.46Hz small sharp peak and the 0.06~0.07Hz sidelobe. Besides, through analysis of the segmented marginal spectra (see Figs.9-12), we found that the appearance time of any 0.2Hz anomalous signal in HHT spectra is consistent with that in the marginal spectra. Thus, the anomalous signals prior to large earthquakes could be characterized by the 0.2Hz anomalous peak.

However, the appearance time of an anomalous signal varies and has certain random nature. This might be explained by the following arguments. Several days to several minutes prior to a large earthquake, the stresses in the interior of the Earth built up and reach a critical state, and this thus causes the slow slip of faults. Meanwhile, extrusion between the faults obstructs the slow slip. In this process, the ground vibration is induced and leads to gravity anomaly and propagation of seismic waves, which might be detected by SG and BS records. And the random appearance time of the anomalous signal may result from the uncertainty of the energy release of the fault when its stress reaches a critical state. Alternatively, the faults may release its energy by successive slow slips and a relative steady state before a large earthquake occurs. Both the starting appearance time and the duration of an anomalous signal are not determinable.

In this study, though the anomalous signals prior to the large earthquake were detected by the records of SGs and BSs, they might involve many factors in the source process, which complicates the study of the relationship between the anomalous signals and the large earthquake occurrence. Without doubt, concerning the present topic, we need further investigations.

References

[1] Yao Y, Chen P, Wu H, Zhang S, Peng W (2012) Analysis of ionospheric anomalies before the 2011 Mw 9.0 Japan earthquake. Chinese Science Bulletin 57(5): 500-510.

[2] Oyama KI, Kakinami Y, Liu JY, Abdu MA and Cheng CZ (2011) Latitudinal distribution of anomalous ion density as a precursor of a large earthquake. Journal of Geophysical Research: Space Physics (1978-2012) 116(A4).

[3] Liu JY, Le H, Chen YI, Chen CH, Liu L, Wan W et al. (2011) Observations and simulations of seismoionospheric GPS total electron content anomalies before the 12 January 2010 M7 Haiti earthquake. Journal of Geophysical Research: Space Physics (1978-2012) 116(A4).

[4] Heki K (2011) Ionospheric electron enhancement preceding the 2011 Tohoku-Oki earthquake. Geophysical Research Letters 38(17).

[5] Ryabinin GV, Polyakov YS, Gavrilov VA and Timashev SF (2011) Identification of earthquake precursors in the hydrogeochemical and geoacoustic data for the Kamchatka peninsula by flicker-noise spectroscopy. arXiv preprint arXiv: 1101.1473.

[6] Le H, Liu JY and Liu L (2011) A statistical analysis of ionospheric anomalies before 736 M6.0+ earthquakes during 2002-2010. J. Geophys. Res. 116: A02303.

[7] Hu XG, Hao XG and Xue XX (2010) The analysis of the non-typhoon-induced microseisms before the 2008 Wenchuan earthquake. Chinese J. Geophys. 53(12): 2875–2886.

[8] Afraimovich EL and Astafyeva EI (2008) TEC anomalies-Local TEC changes prior to earthquakes or TEC response to solar and geomagnetic activity changes? Earth Planets Space 60: 961–966.

[9] Dautermann T., Calais E., Haase J., Garrison J.(2007). Investigation of ionospheric electron content variations before earthquakes in southern California, 2003-2004. Journal of Geophysical Research: Solid Earth,112(B2).

[10] Shelly DR, Beroza GC, Ide S, Nakamula S.(2006). Low-frequency earthquakes in Shikoku, Japan and their relationship to episodic tremor and slip. Nature 442(7099): 188–191.

[11] Gu X, Jiang T, Zhang W, Huang W, Chang Z, Shen WB (2014) Anomalous signals before 2011 Tohoku-oki Mw9.1 earthquake detected by superconducting gravimeters and broadband seismometers. Geodesy and Geodynamics, 5(2): 24-32.

[12] Shen WB and Ding H (2013) A case study of detecting anomalous signals prior to the great 2010 Maule earthquake. Geodesy and Geodynamics 4(1): 1-6.

[13] Shen WB, Wang DJ and Hwang C (2011) Anomalous signals prior to Wenchuan earthquake detected by superconducting gravimeter and broadband seismometers records. Journal of Earth Science 22: 640-651.

[14] Hu XG and Hao XG (2008) The short-term anomalies detected by broadband seismographs before the May 12 Wenchuan earthquake, Sichuan, China. Chinese J. Geophys. 51(6): 1726-1734.

[15] Crossley D, Hinderer J (2008) Report of GGP activities to Commission 3, completing 10 years for the worldwide network of superconducting gravimeters. Observing our Changing Earth. Springer Berlin Heidelberg :511-521.

[16] Goodkind JM (1999) The Superconducting Gravimeter. Rev. Sci. Instrum. 70(11): 4131-4152.

[17] Huang NE, Shen Z, Long SR et al. (1998) The empirical mode decomposition and the Hilbert spectrum for nonlinear and non-stationary time series analysis. Proc. Roy. Soc. Lond. A454(1971): 903-995.

[18] Wenzel HG (1996) The nanogal software: Earth tide data processing package ETERNA 3.30. Bull. Inf. Marées Terrestres 124: 9425-9439.

[19] Huang NE and Wu Z (2008) A review on Hilbert-Huang transform: Method and its applications to geophysical studies. Rev. Geophys 46(2): RG2006.

[20] Chen X, Wu Z and Huang NE (2010) The time-dependent intrinsic correlation based on the empirical mode decomposition. Advances in Adaptive Data Analysis 2(02): 233-265.

[21] Huang NE, Wu Z, Long SR et al. (2009) On instantaneous frequency. Advances in Adaptive Data Analysis 1(2): 177-229.

[22] Huang NE, Wu MLC, Long SR et al. (2003) A confidence limit for the empirical mode decomposition and Hilbert spectral analysis[J]. Proc. Roy. Soc. Lond. A459(2037): 2317-2345.